Journal of Materials Science and Engineering with Advanced Technology
Volume 6, Number 1-2, 2012, Pages 47-69

INFILTRATION OF NANO-SiC-Al_2O_3 AND NANO-SiC-SiO_2 PREFORMS USING AN Al-Si-Mg ALLOY

M. RODRÍGUEZ-REYES[1], H. F. LÓPEZ[2], J. R. PARGA-TORRES[1], J. A. DÍAZ-GUILLEN[1], J. A. AGUILAR-MARTÍNEZ[3] and M. M. CISNEROS[4]

[1]Instituto Tecnológico de Saltillo
Venustiano Carranza 2400
Col. Tecnológico C. P. 25280
Saltillo, Coahuila
México

[2]University of Wisconsin-Milwaukee
3200N, Cramer
Milwaukee, WI 53211
USA
e-mail: hlopez@uwm.edu

[3]Centro de Investigación en Materiales Avanzados
S. C., Alianza Norte 202
Parque de Investigación e Innovación Tecnológica
Nueva Carretera Aeropuerto
Km. 10, C. P. 66600, Apodaca
Nuevo León
México

Keywords and phrases: nano- SiC, nano- Al_2O_3, infiltration, metal matrix nano-composites, aluminum alloys.

Received November 11, 2012

[4]Instituto Tecnológico de Nuevo León
Av. Eloy Cavazos No. 2001
Cd. Guadalupe, C. P. 67170
Nuevo León
México

Abstract

In this work, nano-ceramic preforms containing either SiC/Al_2O_3 or SiC/SiO_2 were infiltrated by using an Al-Si-Mg alloy via pressureless reactive infiltration. In both systems, a relatively large fraction of the nano-reinforcements were exposed to reaction with the molten alloy. It was found that Mg in the vapour phase or in the Al-Si-Mg melt acts to reduce the Al_2O_3 or SiO_2 nanoparticles. Also, when a nitrogen atmosphere is present, Mg_3N_2 is formed. Other reactions occur that result in the formation of $MgAl_2O_4$, AlN including amorphous Al-Mg-Si-O phases. It was found that the Al_4C_3 phase always forms in the SiC/Al_2O_3 system, which can be detrimental for the stability and properties of the reinforced composite. In contrast, in the SiC/SiO_2, the Al_4C_3 phase did not develop probably due to the presence of SiO_2, which inhibits its formation. In addition, reduced infiltration was observed in the SiC/Al_2O_3 system due to the presence of MgO and Al_2O_3. These phases possess low wettability and can make the infiltration process increasingly difficult. In contrast, the $Al/SiC/SiO_2$ exhibited improved metal flow probably as a result of reactive infiltration between the amorphous SiO_2 nanoparticles when in contact with the molten metal. Finally, micro-hardness measurements indicated that these systems exhibit similar values for a given fraction of reinforcement regardless of the type and/or distribution of nanoparticles.

1. Introduction

In recent years, increasing environmental concerns have been forcing the automotive sector into the development of highly fuel efficient ecological vehicles. A key factor in the design of these vehicles is the development of low density materials with unique properties [1, 7, 14, 28]. Among the materials of interest are Al-matrix materials reinforced with diverse ceramic compounds, such as Al_2O_3 or SiC particles [1, 12, 16, 21, 26].

Yet, large scale applications using composite materials is limited due to processing constraints. Among these constraints are (a) reinforcement-matrix reactivity; (b) reduced infiltration velocities; and (c) high processing costs. Despite these limitations, it has been found that the benefits related to weight reduction coupled with improved properties can easily surpass any potential processing shortcomings [7, 15, 26].

Alternatively, there have been various efforts in the development of composite materials consisting of metallic matrices, such as Al-based alloys containing ceramic nano-reinforcements. However, addition of nano-ceramic reinforcements into the melt is not an easy task. Typically, nano-ceramic reinforcements tend to agglomerate resulting in non-uniform nanoparticle distributions in the Al-matrix. Various processing techniques have been suggested including ultrasound in order to promote uniform particle distributions [12]. However, the volume fractions of nanoparticles introduced in a uniform manner are rather low (typically below 1.0wt%). At these nano-reinforcement levels, the tensile strength of an A356 Al-alloy containing SiC nanoparticles has been found to exhibit improvements of nearly 100% with no negative effects to elongation [12]. Yet, beyond 1.0wt% nanoparticle additions, the matrix viscosity increases significantly making processing rather difficult.

Another important constraint is related to the stability and reactivity of nanoparticles in the liquid metal. Hence, alternative processing methods such as pressureless infiltration, which can introduce relatively large volume fractions of reinforcements are highly attractive. Accordingly, in this work, an Al-Si-Mg alloy is used to infiltrate various preforms made of either nano-SiC-Al_2O_3 or nano-SiC-SiO_2. In addition, Mg is introduced into the alloy system in order to investigate its role on the resultant phases developed during alloy infiltration.

2. Experimental

The ceramic nanoparticles employed in this work are SiC, Al_2O_3, and SiO_2. From these nanoparticles, 4cm × 3cm × 0.5cm rectangular preforms containing 40vol% and 25vol% total ceramic reinforcements were prepared by using 10wt% dextrin and 1ml distilled water. The powder mixture was placed in a steel die to compact performs with 60% and 75% porosity. The preforms were dried at 130ºC and cured at 230ºC for 1.5h. For infiltration purposes, the preforms were cut half way. Table 1 gives the vol% of ceramic nanoparticles used in the preform components.

Table 1. Vol% of nano-reinforcements in the investigated systems

System	1 (SiC / Al_2O_3)		2 (SiC / SiO_2)		3 (SiC / Al_2O_3)		4 (SiC / SiO_2)	
Amount	60	40	60	40	60	40	60	40
Preform	40		40		25		25	

The alloy used for preform infiltration purposes was an Al-10Mg-12Si alloy. Prior to pouring the alloy into molds, samples were taken for chemical analyses. Preform infiltration was achieved by placing the preform together with enough amount of Al alloy (40-50g) in a ceramic mold. The system (metal-preform) was heated at 1100ºC for 60 minutes in a high temperature tubular furnace under an N_2 atmosphere in order to promote infiltration. Afterwards, the infiltrated preforms were characterized by using a Philips 3040 diffractometer and a Nova nano SEM scanning electron microscope (SEM) 200 FEI equipped with an energy dispersive X-ray spectroscope (EDX). Finally, micro-hardness measurements were made on the infiltrated preforms.

3. Results and Discussion

3.1. Nano-particle effects

Two groups of nano-α-SiC were identified (spatial group P63mc), which are 4H and 6H (see Figure 1(a)). In both groups, the crystal structure is hexagonal with lattice parameters a = 0.3081nm and c = 1.509nm (group 6H) and a = 0.3073nm and c = 1.005nm (group 4H) [8, 13, 27]. The Al_2O_3 nanoparticles are shown in Figure 1(b), as well as their corresponding diffraction patterns. X-ray diffraction indicated that the crystal structure of Al_2O_3 nanoparticles was cubic and corresponded to γ-Al_2O_3 (spatial group Fd-3m) with a lattice parameter a = 0.7906nm.

In the case of SiO_2 nanoparticles, it was found that it did not exhibit a crystal structure. Figure 1(c) shows a typical X-ray diffraction pattern corresponding to amorphous SiO_2 in a 15-30° 2θ scan. Figures 2(a)-(c) are SEM micrographs of the various nanoparticles employed in this work. Notice that the nanoparticles are agglomerated in all the cases and that average nanoparticle sizes are below 500nm.

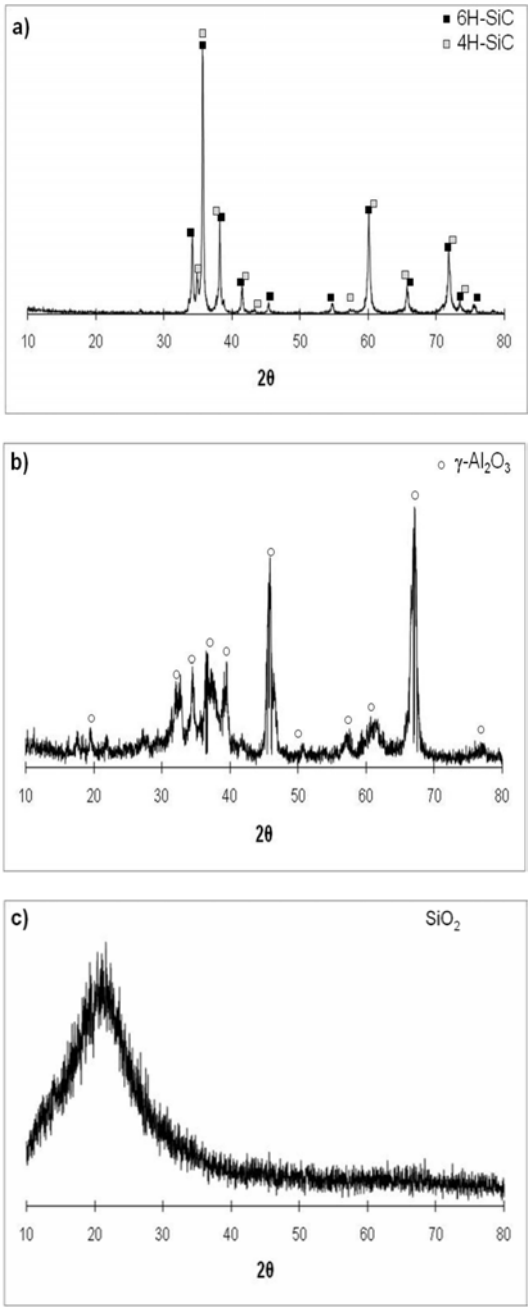

Figure 1. X-ray diffraction patterns of nanoparticles: (a) SiC; (b) Al_2O_3; and (c) SiO_2.

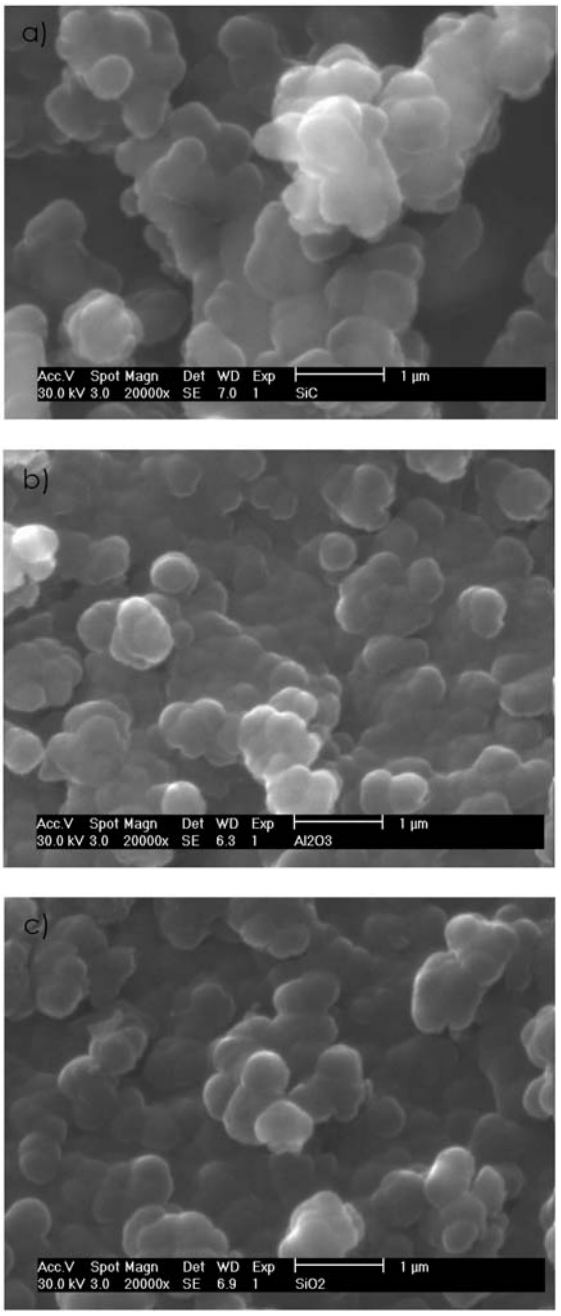

Figure 2. SEM micrographs showing the morphology of nanoparticles: (a) SiC; (b) Al_2O_3; and (c) SiO_2.

Upon melt infiltration, it was found that the nanoceramic reinforcements in the preforms were not stable enough and reacted rapidly with the molten metal. Apparently, the nanoparticles provided a relatively large surface to volumen ratio for enhanced reaction, as well as numerous reaction sites. As a result, new phases formed in relatively short times in the investigated systems. In general, these phases were highly uniform and with a relatively fine grain size structure.

However, melt infiltration was hindered whenever relatively coarse MgO phases developed in the investigated systems. In this preliminary work, there was no attempt to investigate the kinetic aspects of melt infiltration as there are various published works in this field [15, 21]. Instead, the experimental outcome on the infiltrated preforms was focused on the phases developed and their effect of the preform infiltration process.

3.2. SiC/Al_2O_3 preforms

Figure 3 shows SEM micrographs of the SiC/Al_2O_3 infiltrated system, including EDX mapping of the various elements present in the reinforced material. It is apparent from these micrographs, that a predominant dark gray phase develops, which is rich in Mg, O, and N and it is surrounded by the matrix elements (Al and Si). In addition, the isolated porosity was identified with sizes of up to $20\mu m$ in diameter. In order to identify the various phases developed, the Al-metal matrix was chemically removed by using an aqueous solution of KOH (20vol%). Figure 4 shows the remaining phases in the $Al/SiC/Al_2O_3$ infiltrated preform after matrix removal. Semi-quantitative EDX determinations of the elements present at various locations (1-5) were made and are given in Table 2.

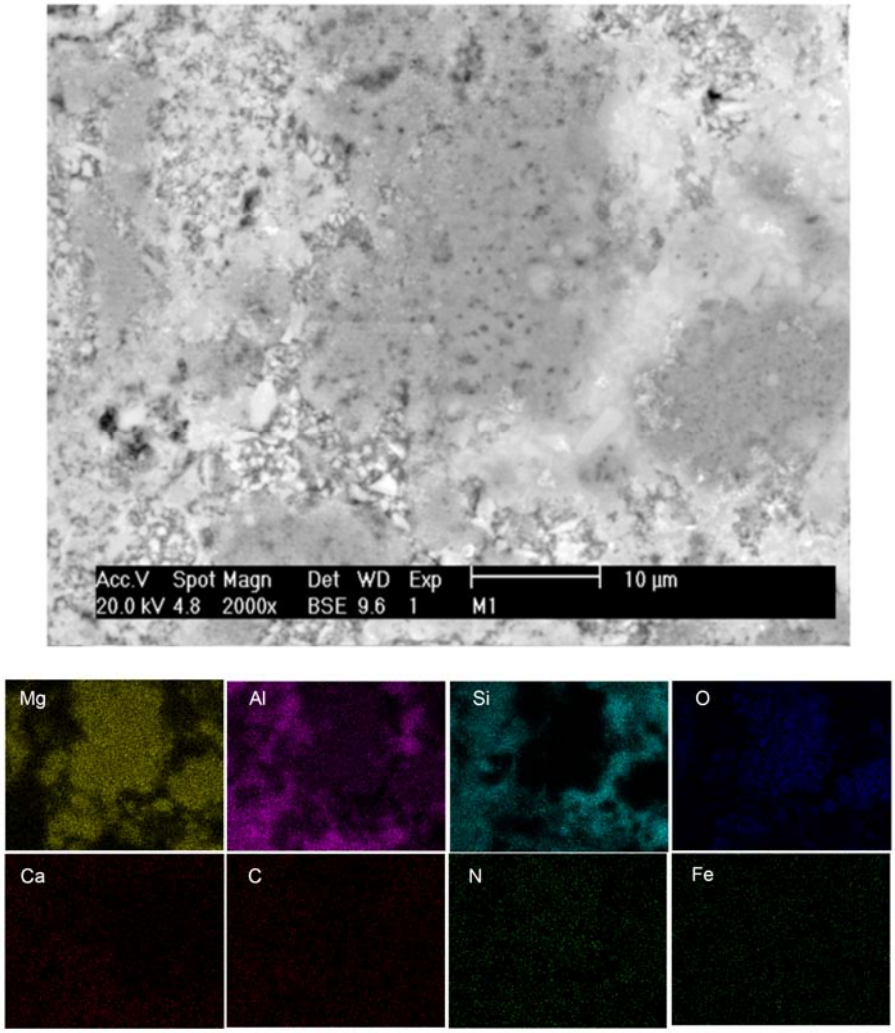

Figure 3. SEM micrograph and X-ray element mapping in the Al/SiC/Al_2O_3 composite.

Table 2. Semi-quantitative EDX determinations (system: $Al/SiC/Al_2O_3$)

	Wt%				
Element	Zone 1	Zone 2	Zone 3	Zone 4	Zone 5
C	32	29		26	
O	35	28	55	34	60
Mg	2	2	14	7.5	9
Al	3	9	5	4	
Si	28	32	0.5	28.5	10
K			23.5		21
Na			2		
Total	100	100	100	100	100

Once again, it is evident from Figure 4, the presence of a relatively coarse and dominant phase (locations 3 and 5), which is rich in Mg and O. In addition, a carbon rich phase is found at locations 1, 2, and 4. Determinations using X-ray diffraction (see Figure 5) identified the resultant phases as SiC, AlN, MgO, and Al_4C_3. Apparently, most of the SiC nano-particles were eliminated through reactive infiltration with the molten Al-alloy giving rise to Al_4C_3 according to the reaction [5, 6, 10, 25].

$$4Al_{(l)} + 3SiC_{(s)} \rightarrow Al_4C_{3(s)} + 3Si_{(in\,Al)} \qquad (1)$$

$$\Delta G_{1100^{\circ}C} = -256 kJ / mol.$$

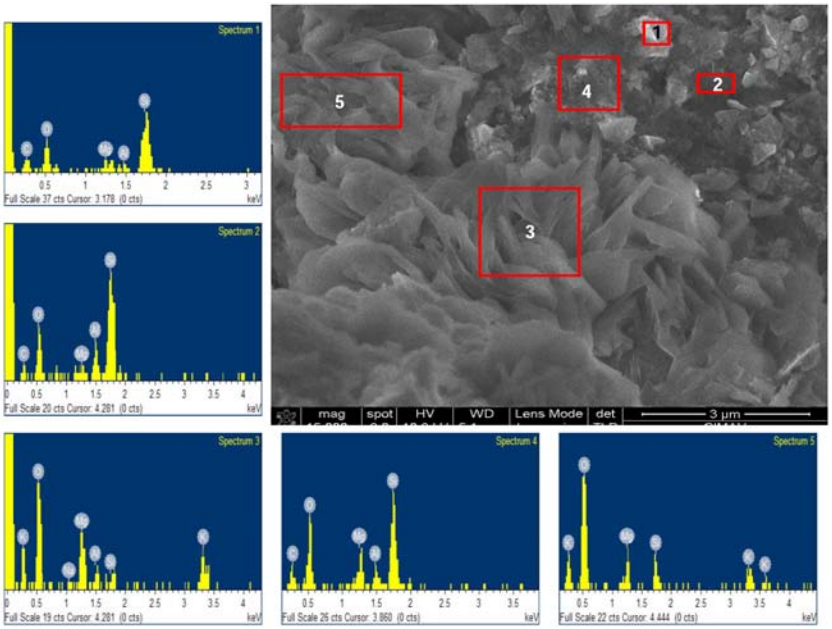

Figure 4. SEM micrograph and EDX spectra showing the morphology and composition at various locations in the $Al/SiC/Al_2O_3$ composite.

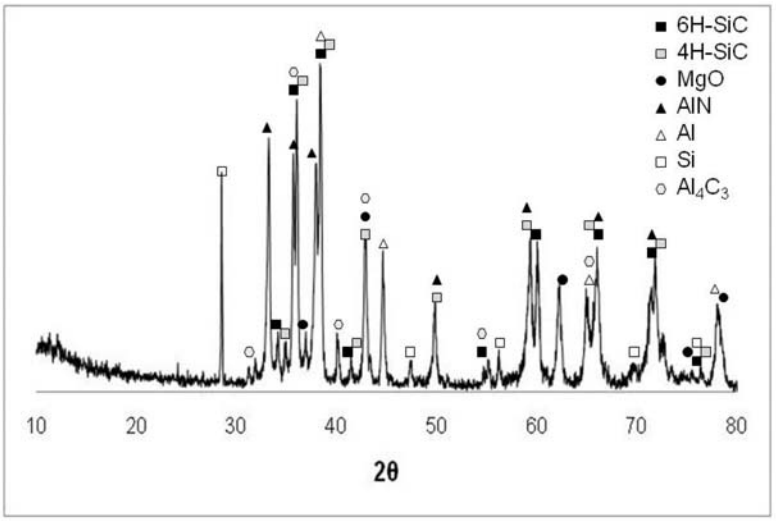

Figure 5. X-ray diffraction peaks of the various phases formed in $Al / SiC/Al_2O_3$ composites.

It is known [19] that the Al_4C_3 phase is considered to be detrimental to the integrity and properties of reinforced Al-composites as it is prone to react with the moisture of the environment as

$$Al_4C_{3(s)} + 18H_2O_{(l)} \rightarrow 4Al(OH)_{3(s)} + 3CO_{2(g)} + 12H_{2(g)}. \quad (2)$$

As a result of this reaction, there can be significant degradation of the reinforced material as appreciable swelling is known to occur, particularly at the matrix-reinforcement interfaces [5, 6, 10, 25]. In this work, infiltration was carried out under a nitrogen atmosphere. Hence, the development of AlN can be attributed to reaction of nitrogen with the molten alloy according to the following reactions [11]:

$$3Mg_{(g)} + 2[N] \rightarrow Mg_3N_{2(s)} \quad (3)$$

$$\Delta G_{1100^\circ C} = -175 kJ/mol;$$

$$Mg_3N_{2(s)} + 2Al_{(l)} \rightarrow 2AlN_{(s)} + 3Mg_{(l)} \quad (4)$$

$$\Delta G_{1100^\circ C} = -175 kJ/mol.$$

In addition, MgO is expected to form due to reduction of Al_2O_3 with Mg vapourization from the liquid melt (see reaction below). In general, it is found that MgO forms when the Mg concentration is in the range of 2 to 5 wt% at temperatures of or above 650°C [17, 18, 24].

$$2Mg_{(v)} + Al_2O_3 \rightarrow 3MgO + 2Al \quad (5)$$

$$\Delta G_{350^\circ C} = -167 kJ/mol.$$

In an attempt to identify the active phase formation reactions, non-infiltrated preforms were subject to air at 1100°C for 60 minutes and the resultant phases identified by X-ray diffraction. Figure 6 shows the various phases identified by these means (SiC, Al_2O_3, MgO, and $MgAl_2O_4$). Notice that in this case, no AlN phases developed.

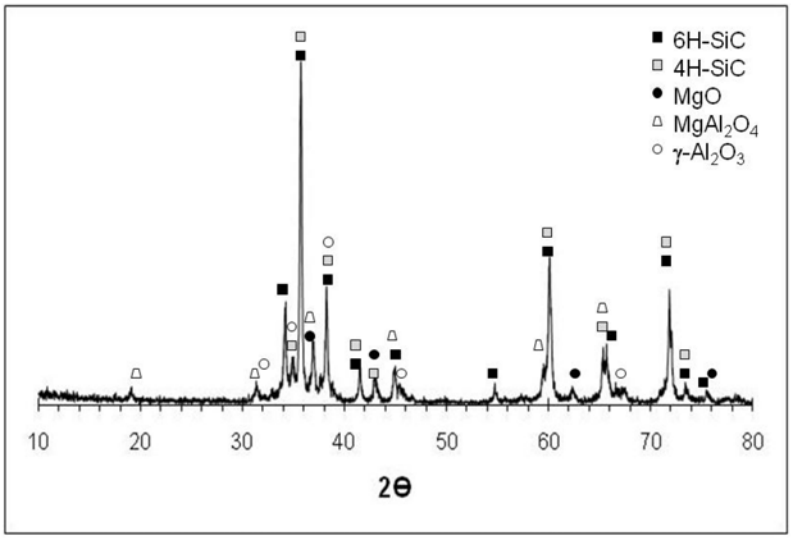

Figure 6. X-ray diffraction peaks of SiC/Al_2O_3 preforms processed at 1100°C for 60 min.

Moreover, no Al_4C_3 was found to form probably due to the lack of molten Al infiltration into the preform. MgO was present suggesting that reaction (5) was active under these conditions. In addition, the MgO phase promoted the formation of $MgAl_2O_4$ spinel through reaction between Al_2O_3 and MgO, according to [13, 17, 18, 24]

$$Al_2O_{3(s)} + MgO_{(s)} \rightarrow MgAl_2O_{4(s)} \quad (6)$$

$$\Delta G_{(827°C)} = -47.6 kJ/mol.$$

3.3. SiC/SiO_2 preforms

A similar experimental analysis to the one in the previous section (SiC/Al_2O_3 preforms) was carried out on the SiC/SiO_2 system. Once again, notice the development of relatively fine new phases through melt reaction with the nano-sized ceramic reinforcements. Figure 7 is an SEM micrograph of the resultant microstructure including EDX mapping of the various elements involved. Apparently, the light gray phases are made up of mostly Al and Si corresponding to the Al-alloy, whereas the

dark gray phase consists mostly of Al, Mg, and O. Just as in the previous system, the isolated porosity with an average size of 10μm was found in this system.

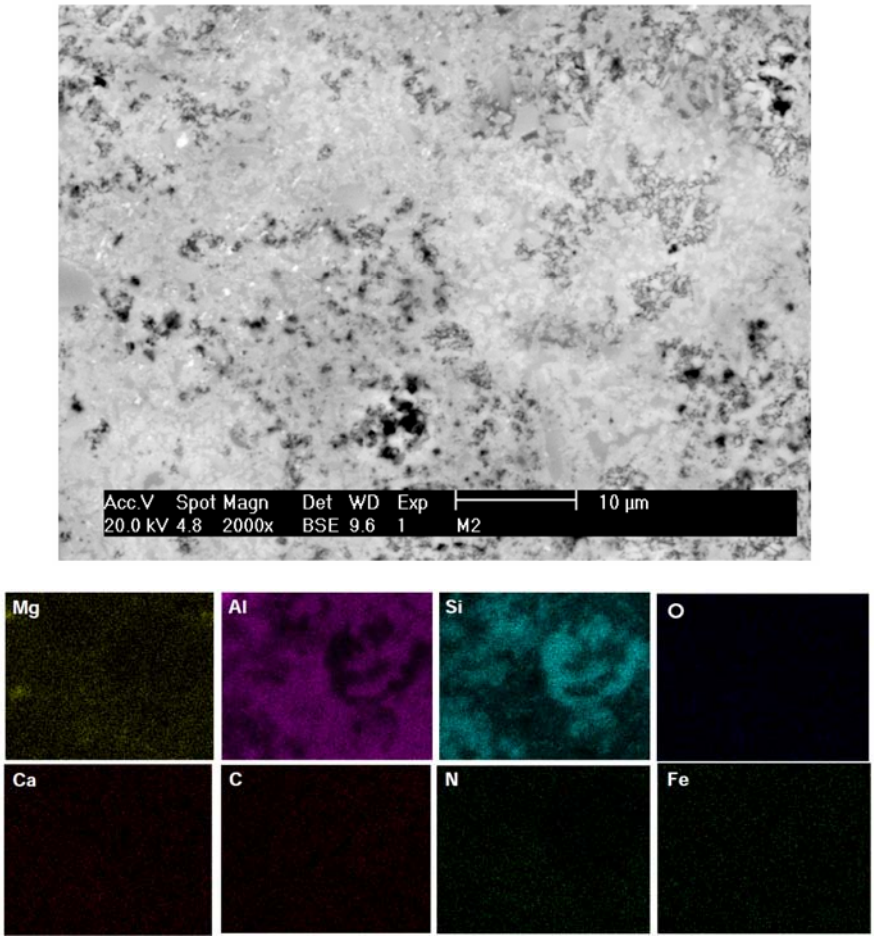

Figure 7. SEM micrograph and X-ray element mapping in the $Al/SiC/SiO_2$ composite.

After removal of the metallic matrix in the SiC/SiO_2 system, elemental EDX determinations of composition were made at various locations (1 to 5) and they are given in Table 3. In this table, locations 1 and 5 correspond to relatively fine phases rich in Mg and O. At locations

2 and 3, an Al and O rich phase is found and at location 5, an Si-O rich phase is present. Identification by X-ray diffraction indicated that the resultant phases in this system correspond to SiC, MgO, and AlN. It was not possible to detect any other phases using X-ray diffraction due to their amorphous nature. Nevertheless, there are reports indicating that SiO_2 particles can also react with the Al-melt to form aluminosilicates [26], which might be the case at location 5 (see Figure 9). Also, notice that in this system AlN phases were formed, whereas the development of Al_4C_3 phases was avoided.

Table 3. Semi-quantitative EDX determinations (system: $Al/SiC/SiO_2$)

	Wt%				
Element	Zone 1	Zone 2	Zone 3	Zone 4	Zone 5
C	9.87				
O	45.5	8.72	18.21	16.16	41.02
Mg	2.53	0.62			3.6
Al	14.62	59.88	58.36	18.53	14.32
Si	21.44	5.39	23.43	38.03	29.3
K	6.04			27.28	11.76
Na					
N		25.39			
Total	100	100	100	100	100

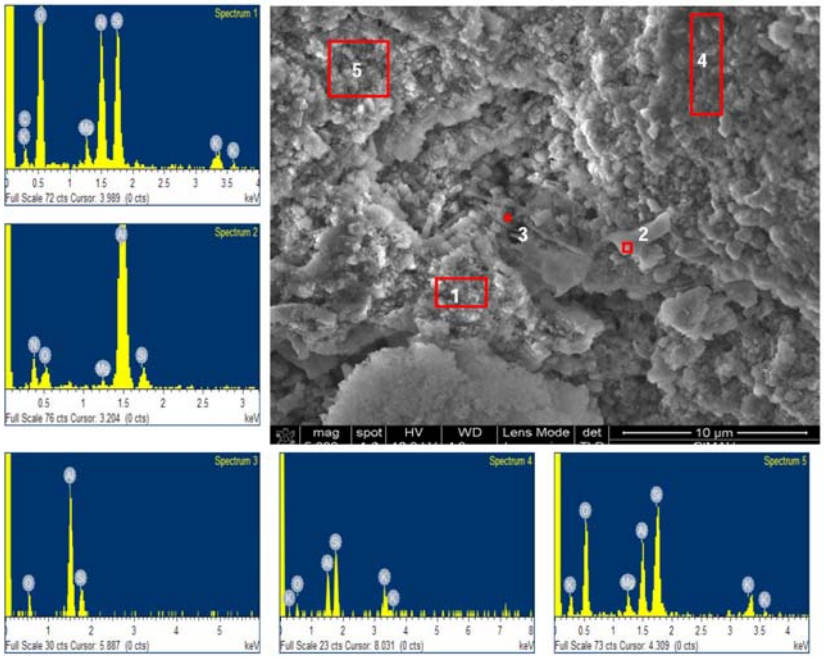

Figure 8. SEM micrograph and EDX spectra showing the morphology and composition at various locations in the $Al/SiC/SiO_2$ composite.

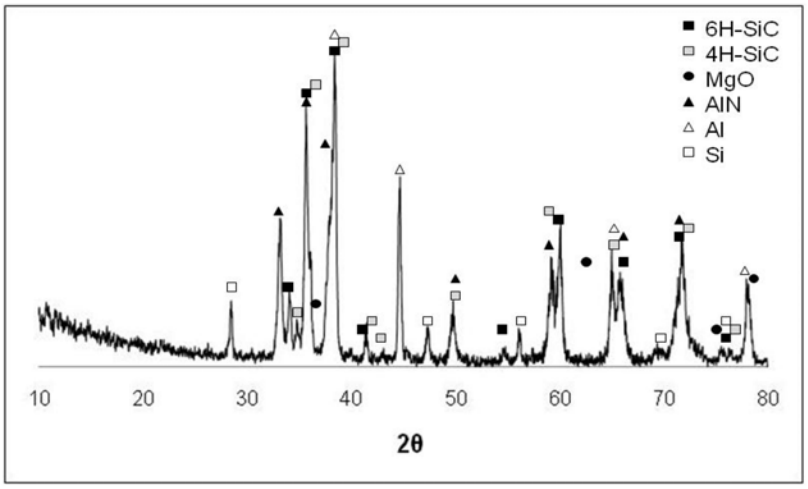

Figure 9. X-ray diffraction peaks of $Al/SiC/SiO_2$ composites processed at 1100°C for 60 min.

In non-infiltrated preforms exposed at 1100°C for 60 minutes, the resultant phases identified by X-ray diffraction were SiC and MgO (see Figure 10). The presence of MgO in the $Al/SiC/SiO_2$ system can be attributed to reaction of the SiO_2 nanoparticles with Mg in the vapour phase according to

$$SiO_{2(s)} + 2Mg_{(v)} \rightarrow 2MgO_{(s)} + Si_{(s)} \quad (7)$$

$$\Delta G_{(1100°C)} = -230 kJ/mol.$$

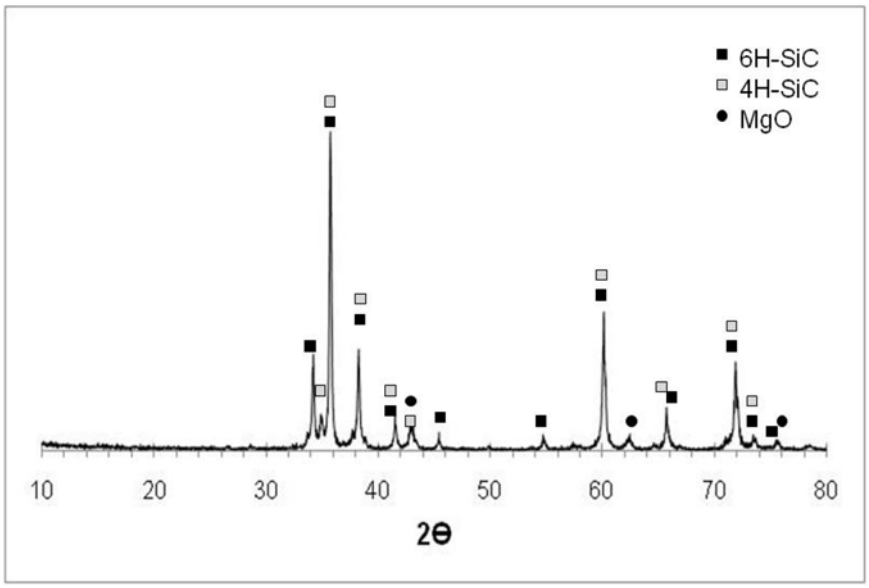

Figure 10. X-ray diffraction peaks of SiC/SiO_2 preforms processed at 1100°C for 60 min.

From the experimental outcome, two stages can be envisaged in the processing of these composites. (a) Prior to infiltration with the molten alloy in both preforms investigated, the Al_2O_3 or SiO_2 nanoparticles are partly reduced by Mg in the vapour phase to form MgO. Due to its low vapour pressure, magnesium is lost by evaporation from the Al-Si-Mg alloy; part of the Mg vapour condenses on the furnace walls as Mg, MgO

or Mg_3N_2 and part of it is removed by the nitrogen flow [20]. In addition, Mg_3N_2 phases develop through reaction with the nitrogen atmosphere. (b) Additional reactions occur through infiltration of the Al-melt into the ceramic preforms that can give rise to either AlN, MgO, Al_4C_3, and amorphous Al-Mg-Si-O phases.

Notice that the use of nitrogen atmospheres is helpful in promoting the infiltration of the Al-melt through porous preforms. In particular, nitrogen favours the formation of AlN, which can be considered as a reinforcing phase in the system due to its inherent thermal and structural properties. Moreover, no Mg_2Si phases were detected in the experimental composites. It is well known that Mg_2Si is highly undesirable as it promotes pitting corrosion in metal-matrix composite materials [2, 4].

3.4. Degree of infiltration

Figure 11 is a comparative chart on the degree of infiltration in the investigated systems, SiC/Al_2O_3 (40vol% and 25vol% ceramic component) and SiC/SiO_2 (40vol% and 25vol% ceramic component). Notice that systems 1 and 3 exhibit a reduced degree of infiltration (between 15% to 30%) when compared with systems 2 and 4, which do not contain Al_2O_3 nanoparticles (65-100% infiltration). Apparently, the degree of infiltration in the $Al/SiC/Al_2O_3$ is adversely influenced by the presence of Al_2O_3 and a relatively coarse MgO phase. These phases exhibit poor wettability and can explain the reduced degree of infiltration [3, 9, 22, 23, 29]. Moreover, a reduced infiltration coupled with the development of Al_4C_3 can be considered highly restricting factors in the processing of in the SiC/Al_2O_3 composites.

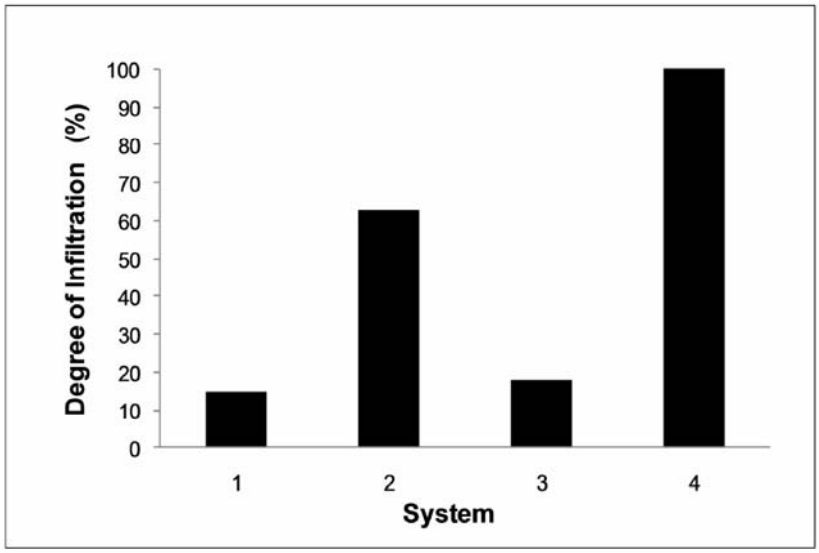

Figure 11. Degree of infiltration in (1) $Al/SiC/Al_2O_3$ (40vol% ceramic component); (2) $Al/SiC/SiO_2$ (40vol% ceramic component); (3) $Al/SiC/Al_2O_3$ (25vol% ceramic component); and (4) $Al/SiC/SiO_2$ (25vol% ceramic component).

In contrast, the SiC/SiO_2 exhibits relatively good infiltration properties. Apparently, the presence of amorphous nano-SiO_2 phase in contact with the Al-alloy melt promotes metal flow through reactive infiltration. In addition, the morphology of the resultant MgO phase was rather fine and their relative amounts rather small to play a dominant role on hindering melt infiltration (see Tables 2 and 3).

3.5. Vickers hardness

Figure 12 shows the resultant hardness values in the investigated preforms. Notice that systems 1 (SiC/Al_2O_3) and 2 (SiC/SiO_2) contain 40vol% ceramic reinforcements, whereas systems 3 (SiC/Al_2O_3) and 4 (SiC/SiO_2) contain 25vol%. In all the systems, the exhibited hardness values do not seem to be influenced by the type of phases developed nor by the degree of infiltration, but by the volume

fraction of reinforcements. In systems 1 and 2, the exhibited hardness is 600kg/mm^2, but it drops down to 500kg/mm^2 when the volume percent of ceramic reinforcements is reduced to 25%.

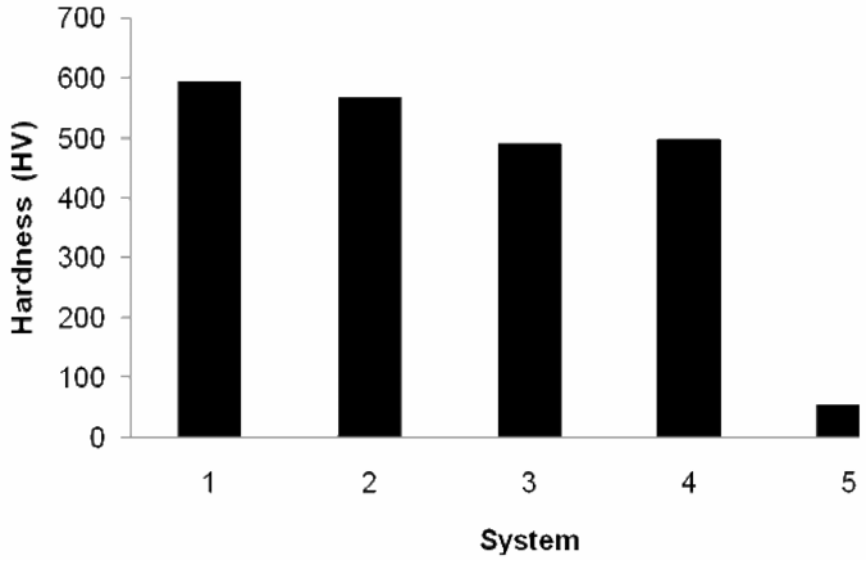

Figure 12. Vickers hardness for composites (1) $\text{Al} / \text{SiC} / \text{Al}_2\text{O}_3$ (40vol% ceramic component); (2) $\text{Al} / \text{SiC} / \text{SiO}_2$ (40vol% ceramic component); (3) $\text{Al} / \text{SiC} / \text{Al}_2\text{O}_3$ (25vol% ceramic component); (4) Al/SiC/SiO_2 (25vol% ceramic component); and (5) Al-Si-Mg alloy.

4. Conclusions

(1) In the systems investigated ($\text{SiC} / \text{Al}_2\text{O}_3$ and $\text{SiC} / \text{SiO}_2$ preforms), a relatively large fraction of nano-ceramic reinforcements was rapidly consumed through reaction with the molten metal.

(2) Mg plays an important role in processing nano-composite preforms via infiltration as it acts either in the vapour or liquid phase to reduce the Al_2O_3 or SiO_2 nanoparticles. Two stages are found: (a) In stage 1, Mg in the vapour phase partially reduces the Al_2O_3 and SiO_2

nanoparticles to form MgO. Also, in the presence of a nitrogen atmosphere, Mg_3N_2 can be formed. (b) In stage 2, during melt infiltration additional reactions give rise to the formation $MgAl_2O_4$, AlN as well as amorphous Al-Mg-Si-O phases.

(3) In this work, the Al_4C_3 phase was found to form in the SiC/Al_2O_3 system, which is detrimental for the stability and properties of the reinforced composite. In the SiC/SiO_2, the Al_4C_3 phase did not form probably due to the presence of SiO_2, which inhibits its formation.

(4) The degree of infiltration is severely hindered in SiC/Al_2O_3 systems probably due to the presence of relatively coarse MgO and Al_2O_3. These phases possess low wettability and can make the infiltration process increasingly difficult. In contrast, the SiC/SiO_2 exhibited improved metal flow probably as a result of reactive infiltration between SiO_2 when in contact with the molten metal.

(5) Vickers hardness measurements in the systems containing 40vol% and 25vol% ceramic reinforcements indicated that hardness exhibits similar values for a given amount of reinforcement and that it drops by $100kg/mm^2$ when the amount of reinforcement is reduced by 15vol%.

Acknowledgement

The authors are grateful to Mrs. N. Pineda-Aguilar and M. Sneider Alcala for their technical support.

References

[1] Aluminum and Aluminum Alloys, Aluminum-matrix composites, ASM Specialty Handbook (1998), 160-179.

[2] S. Candan and E. Bilgic, Materials Letters 58 (2004), 2787-2790.

[3] J. Chen, M. Gu and F. Pan, J. Mats. Res. 17 (2002), 911-917.

[4] J. H. W. De Wit, Electrochimica Acta 49 (2004), 2841-2850.

[5] T. Fan, K. Zhang, Z. Shi, R. Wu, T. Shibayangai, M. Naka and H. Mori, J. Mats. Sci. 34 (1999), 5175-5180.

[6] K. Guerfi, S. Lagerge, M. J. Meziani, Y. Nedellec and G. Chauveteau, Thermochimica Acta 434 (2005), 140-149.

[7] S. F. Hassan and M. Gupta, Composite Structures 72 (2006), 16-26.

[8] B. Jin, W. Zhang, G. Sun and H. B. Gu, J. Ceramic Processing Res. 8(5) (2007), 336-340.

[9] J. C. Lee, K. N. Subramanian and Y. Kim, J. Mats. Sci. 29 (1994), 1983-1990.

[10] J. C. Lee, J. P. Ahn, Z. Shi, Y. Kim and H. I. Lee, Met. Mat. Trans. A 31A (2000), 2361-2368.

[11] J. G. Legoux, L. Salvo, H. Ribes, G. L'Esperance and M. Suery, Interfaces in metal-ceramics composites, The Minerals, Metals & Materials Society (1989), 187-196.

[12] X. Li, Y. Yang and D. Weiss, AFS Trans., Schaumburg, IL USA, (2007), 1-12.

[13] X. Liu, Z. Wu, T. Peng, P. Cai, H. Lv and W. Lian, Mat. Res. Bull. 44 (2009), 160-167.

[14] L. Lu, K. K. Thong and M. Gupta, Composites Sci. and Tech. 63 (2003), 627-632.

[15] Z. P. Luo, Y. G. Song and S. Q. Zhang, Scripta Mat. 45 (2001), 1183-1189.

[16] Z. P. Luo, Acta Mater. 54 (2006), 47-58.

[17] A. D. McLeod and C. M. Gabryel, Metall. Trans. A 23A (1992), 1279-1283.

[18] B. C. Pai, G. Ramani, R. M. Pillai and G. Satyanarayana, J. Mats. Sci. 30 (1995), 1903-1911.

[19] J. K. Park and J. P. Lucas, Scripta Mat. 37(4) (1997), 511-516.

[20] M. Rodriguez-Reyes, M. I. Pech-Canul, E. E. Parras-Medecigo and A. Gorokhowsky, Materials Letters 57 (2003), 2081-2089.

[21] N. Shao, J. E. Dai, G. Y. Li, H. Nakae and T. Hane, Materials Letters 58 (2004), 2041-2044.

[22] P. Shen, H. Fuji, T. Matsumoto and K. Nogi, Acta Mater. 52 (2004), 887-898.

[23] N. Sobczac, R. Asthana, M. Ksiazek, W. Radziwill and B. Mikulowski, Metall. Mat. Trans. A 35A (2004), 911-923.

[24] B. Srinivasa Rao and V. Jayaram, Acta Mat. 49 (2001), 2373-2385.

[25] J. Suda and M. Horita, Mats. Res. Soc. Bull. 34(5) (2009), 348-352.

[26] A. Urena, M. D. Escalera, P. Rodrigo, J. L. Baldonero and L. Gil, J. Microscopy 201 (2001), 122-136.

[27] M. Villegas, T. Sierra, A. C. Caballero and J. F. Fernandez, Ceramics Int. 33 (2007), 875-878.

[28] G. Y. Yuan, Z. L. Liu, Q. D. Wang and W. J. Ding, Materials Letters 56 (2002), 53-58.

[29] X. B. Zhou and T. M. De Hosson, Acta Mater. 44 (1996), 421-426.

■